Evaluation at 290°C and 8 MPa of the Anticorrosion Properties of Hydrothermal Ceramic Nanodeposits on Preoxidized 304L SS.

N. López-García[1, 2], M. Marín-Almazo, A. L. Medina-Almazán
[1] Instituto Nacional de Investigaciones Nucleares
Carretera México-Toluca s/n, La Marquesa, Ocoyoacac, Estado de México, C.P. 52750, México
natali_log@hotmail.com; margarita.marin@inin.gob.mx; liliana.medina@inin.gob.mx

G. Galicia-Aguilar
[2] Instituto de Ingeniería/Universidad Veracruzana
Av. Juan Pablo II s/n, Fracc. Costa Verde, Boca del Río, Ver., C.P. 94294, México
gogalicia@uv.mx

Abstract

In the present paper, we present the electrochemical evaluation carried out under reductive conditions (molar ratio H_2:O_2 >5), at 290°C and 8MPa, of preoxidized 304L SS with hydrothermal deposits of nanoparticles of TiO_2 and ZrO_2. The anticorrosion properties of the deposits were studied by Electrochemical Impedance Spectroscopy (EIS) and Linear Polarization Resistance (LPR). After electrochemical tests, the samples were characterized by X-Ray Diffraction (XRD) and Scanning Electron Microcopy (SEM). It was found by EIS that both, ZrO_2 and TiO_2 produce an increase in the charge transfer resistance (R_{CT}) of preoxidized 304L SS. At the same time, by LPR we observed that the studied ceramic nanodeposits decrease the corrosion rate (CR) and corrosion current density (i_{corr}), however, in most of the cases the Electrochemical Corrosion Potential (ECP) is slightly higher in the presence of the ceramic nanodeposits than the one of preoxidized 304L SS. After holding time at 290°C, when the impedance (Z) increases, the capacitance increases also, which is attributed to a surface increase due to the roughness of the oxide formed at this temperature under a reductive environment. The observed electrochemical behavior has a dependence on the homogeneity and thickness of the deposits, as has been corroborated by SEM and XRD. The best electrochemical results are obtained when two conditions are fulfilled: The bigger the effective coated area and the lower the deposit thickness.

1. INTRODUCTION

For the safe Long Term Operation (LTO), operation beyond the design lifetime, of the existing Nuclear Power Plants (NPP), one of the main issues is the assessment of the performance of its Structures, Systems and Components (SSC) during the period of Extended Operation (EO). In boiling water reactors (BWR), the reactor pressure vessel internals (RPVI) components are submitted to both, Neutron irradiation and high oxidizing environment which lead (together, by itself or mixed with a sensitized condition or work hardening) to stress corrosion cracking (SCC)

[1- 4]. One of the measures to mitigate SCC in BWR is the decrease of the Electrochemical Corrosion Potential (ECP) of the structural materials by the injection of hydrogen, Hydrogen Water Chemistry (HWC, 1-2 ppm H_2), by Noble Metal Chemical Addition (NMCA, 0.1- 0.3 ppm H_2), or by On-Line NobleChem^{TM} (OLNC, lower H_2 concentration) [5]. There also new proposed technologies for getting a lower ECP, such as the Methanol injection during startup and shutdown [6] and ceramic coatings as TiO_2 and ZrO_2 [7]. However, ECP is a thermodynamic measurement that by itself little says about the kinetics of the process of SCC. In this sense, in [8] it is reported that samples treated for having a lower ECP may exhibit higher i_{corr}, higher percentages of Intergranular Stress Corrosion Cracking (IGSCC) and longer crack depths than untreated samples. In the same way, [9] shows that crack growth rate of 304L SS is practically the same in both, HWC (low ECP) and Normal Water Chemistry (NWC, high ECP) conditions.

In the present work, we perform the electrochemical evaluation of TiO_2 and ZrO_2 ceramic coatings, focusing in the thermodynamic (ECP) and kinetic (CR and i_{corr}) parameters that could affect SCC susceptibility of 304L SS at 290°C and 8 MPa. For do that, we utilized nondestructive electrochemical techniques, Linear Polarization Resistance (LPR) and Electrochemical Impedance Spectroscopy (EIS). Such techniques are difficult to carry out in low conductivity media, such as demineralized water, however in this work it was possible to perform them by using a potenciostat with a low current module. LPR and EIS do not cause damage to the sample. That represents an advantage comparing with other electrochemical techniques, such as potentiodynamic polarization, that alter the surface of the sample, doing difficult the comparison between test replicates of the same specimen.

2. METHODOLOGY

2.1. Specimen Preparation

The material used in this work was 304L SS. Its chemical composition is shown in Table I. It was received in the standard metallurgical condition (solution annealing at 1050°C).

Table I. Chemical composition of 304L stainless steel studied (Wt. %, bal. Fe).

Steel	Cr	Ni	C	Si	Mn	P	N	S
304L SS	18.04	8.11	0.02	0.34	1.75	0.069	0.08	0.003

Specimens of 1x1x0.5 cm^3 were obtained from the received plate. They were preoxidized in a recirculation loop during three weeks in pure water containing 4 ppm dissolved O_2 at 290°C and 8 MPa.

2.2. TiO_2 and ZrO_2 deposits

Ceramic nanodeposits were obtained by hydrothermal process using concentrated solutions of nanoparticles of ZrO_2 and TiO_2 (in both phases, Anatase and Rutile). Preoxidized specimens of 304L SS were introduced into 304 SS hexagonal capsules containing the ceramic solutions, then,

the capsules were located in an autoclave filled with high purity water and taken to 150°C during 48 hrs at 2.24 MPa. In Table II are listed the samples studied.

Table II. Sample ID and kind of nanodeposit studied.

Sample ID	Deposit
DL36 Preox	Preoxidized
DL12 ET4-A	TiO_2-Anatase
DL23 ET4-R	TiO_2-Rutile
DL33 ET16-R	
DL35 ET16-R	
DL22 EZ3-M	ZrO_2
DL58 EZ3-M	
DL50 EZ4-M	
DL51 EZ4-M	

2.3. Electrochemical Tests

Electrochemical tests were performed in a loop, comprising a clean-up and water conditioning unit and an autoclave. One water chemistry condition was tested: Molar ratio H_2 : O_2 >5 (less than 10 ppb of dissolved O_2), conductivity 0.18 μS/cm and pH 6.

For monitoring the water chemistry parameters, it was used a WTW 82363 Wilhem Model LF 340 conductivity meter; an Oakton Model DO 300 series oxygen meter; a Cole Parmer Digi Sense pH meter; and a Hach Ultra 510/B00/P1C controller with an Orbisphere 510 hydrogen sensor.

The obtained deposits were electrochemical evaluated at 290°C and 8MPa by EIS and LPR with a potentiostat Bio-logic model SP-150, with a low current module, coupled to a mobile station. LPR electrochemical measurements were performed with a perturbation of ± 20mV and 10mV/min as scan rate. EIS measurements were carried out at open circuit potential, (E_{OC}), in a frequency range from 20KHz to 0.1Hz with 10 mV/rms signal perturbation and 10 points per decade. EIS and LPR techniques were carried out in a three-electrode array at 8 MPa pressure and 290°C. The 304L SS preoxidized specimens (with and without ceramic nanodeposits) were used as working electrode and a Pt mesh as counter electrode. Both electrodes were spot welded to stainless steel wires coated with PTFE for electrical insulation. An external Ag/AgCl reference electrode filled with saturated KCl electrolyte solution was inserted into the autoclave. This reference electrode was calibrated against a standard Calomel reference electrode to ensure its integrity. The measured potential between the reference electrode and the specimen has been converted to the standard hydrogen electrode (SHE) scale.

Two series of tests were performed, the first one after 15 days at 290°C and 8MPa (Test 1), the second one after 26 days in such conditions (Test 2).

2.4. Surface Characterization

After the electrochemical tests, the surface of the specimens was studied with a SEM Jeol JSM 6610LV with an Oxford Energy Dispersive X-Ray (EDX) probe. The XRD characterization was carried out using a Siemens D-5000 diffractometer, with a Cu K_α (λ=1.54178 Å) radiation at 35 kV and 25 mA

3. RESULTS AND DISCUSSION

3.1 Electrochemical Tests

In Figure 1 we present the experimental results obtained from the LRP technique. In Table III and Table IV we report the ECP, Rp, i_{corr} and CR values determined from Figure 1 a) and Figure 1 b) respectively; the CR, i_{corr} and Rp values were computed using Ec-Lab® electrochemistry software. Only one sample has a lower ECP than the preoxidized one, DL35 with rutile deposit, however in the Test 1 it presents a similar electrochemical behavior than the preoxidized sample (DL36) in Rp, i_{corr} and CR. Nevertheless, after a longer time at the studied conditions, it presents the same behavior of the samples DL33 (rutile), DL22 (ZrO_2) and DL58 (ZrO_2), except for the ECP. We remark that samples DL50 and DL51, with the same kind of deposit, present a different behavior between them. This could be attributed, as it will be seen later, to the deposit thickness or the effective coated area. When we compare Figure 1 a) with Figure 1 b) it is observed in general that the samples present a less electronegative ECP as the holding time at 290°C and 8 MPa increases, but in all the cases the ECP (SHE) present very low values, as a consequence of the low content of O_2 in the studied environment.

The EIS measurements were acquired to relate the thickness with the corrosion protection capacity of the deposits or oxide layers obtained. Impedance experimental data are presented in Figure 2, as Nyquist diagrams. Additionally, this technique allows determining the capacitor formed at the interface metal-electrolyte [9, 11]. The capacitance values, reported in Table V and Table VI, were determined from the Brug's equation [12]:

$$C = Q^{1/\alpha}[R_e^{-1} + R_{CT}^{-1}]^{\alpha-1/\alpha} \qquad (1)$$

where:

C= Capacitance
Q = Brug constant
α= Linear parameter from log (frequency) vs log (imaginary Z, Z´´)
R_e= Electrolyte resistance (Ohms)
R_{CT}= Charge transfer resistance (Ohms)

a)

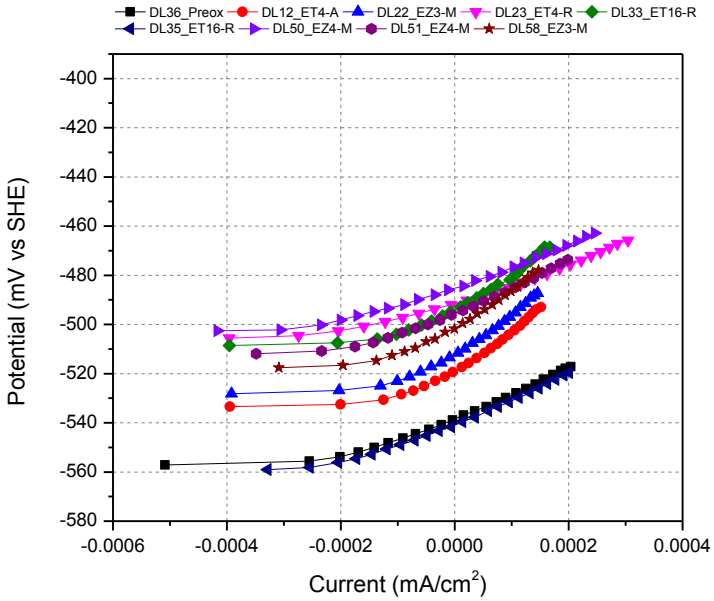

b)

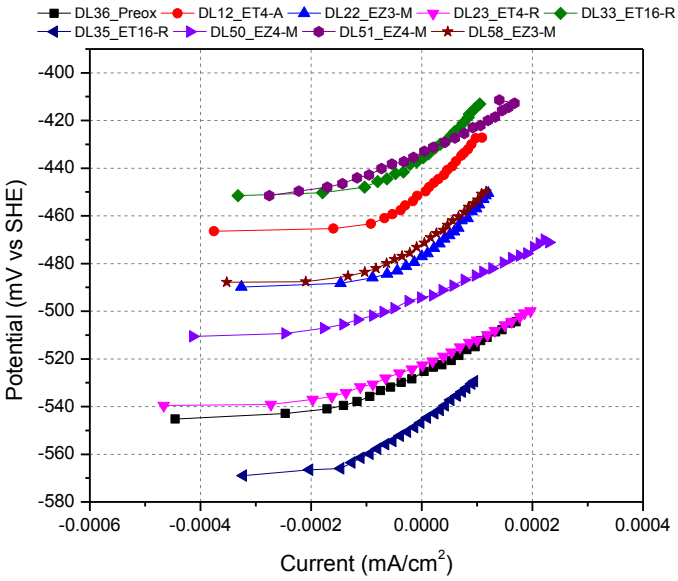

Figure 1. LPR experimental data of preoxidized 304L SS samples tested at 290°C, 8 MPa and Molar ratio H_2 : O_2 >5. a) Test 1; b) Test 2.

Table III. ECP, Rp, i_{corr} and CR of preoxidized 304L SS samples tested at 290°C, 8 MPa and Molar ratio H_2 : O_2 >5. Test 1.

Sample ID	ECP (mV vs SHE)	Rp (kΩ)	i_{corr} (μA/cm^2)	CR (μm/year)
DL36 Preox	-538	91.30	8.90E-2	1.01
DL12 ET4-A	-519	127.07	6.39E-2	0.73
DL23 ET4-R	-492	65.21	1.25E-1	1.41
DL33 ET16-R	-494	117.70	6.90E-2	0.78
DL35 ET16-R	-541	91.64	8.87E-2	1.01
DL22 EZ3-M	-512	131.72	6.17E-2	0.70
DL58 EZ3-M	-502	127.05	6.40E-2	0.73
DL50 EZ4-M	-485	76.15	1.07E-1	1.21
DL51 EZ4-M	-496	95.47	8.51E-2	0.97

Table IV. ECP, Rp, i_{corr} and CR of preoxidized 304L SS samples tested at 290°C, 8 MPa and Molar ratio H_2 : O_2 >5. Test 2.

Sample ID	ECP (mV vs SHE)	Rp (kΩ)	i_{corr} (μA/cm^2)	CR (μm/year)
DL36 Preox	-526	102.27	7.95E-2	0.90
DL12 ET4-A	-451	186.98	4.35E-2	0.49
DL23 ET4-R	-523	86.75	9.37E-2	1.06
DL33 ET16-R	-436	157.13	5.17E-2	0.59
DL35 ET16-R	-546	157.18	5.17E-2	0.59
DL22 EZ3-M	-477	156.31	5.20E-2	0.59
DL58 EZ3-M	-472	154.70	5.25E-2	0.60
DL50 EZ4-M	-494	84.87	9.57E-2	1.09
DL51 EZ4-M	-434	107.73	7.54E-2	0.86

High impedance corresponds to better corrosion properties. From the Nyquist diagrams (Figure 2 a) and Figure 2 b)), it is observed that when holding time at the studied conditions is increased, impedance also rises, consequently R_{TC} increases (see Table V and Table VI). This is explained by an increase in thickness of the oxide formed in such environment. From equation (2), decreasing the capacitance values leads to higher impedance. However, comparing the data of Table V with the one of Table VI, we observe the opposite behavior, when impedance increases, the capacitance also does. This could be explained, per equation (3), due to an increase in the exposed area, which leads to an increase in capacitance values, even if the thickness increases at the same time. The increase of area could be related with the roughness of the oxides formed at the studied environmental conditions.

a)

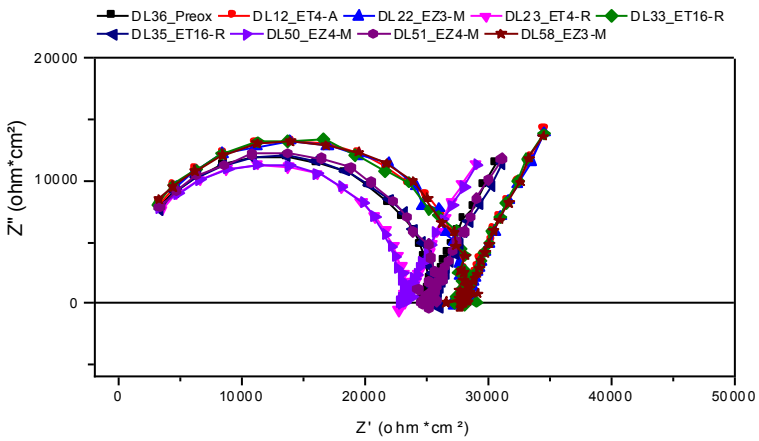

b)

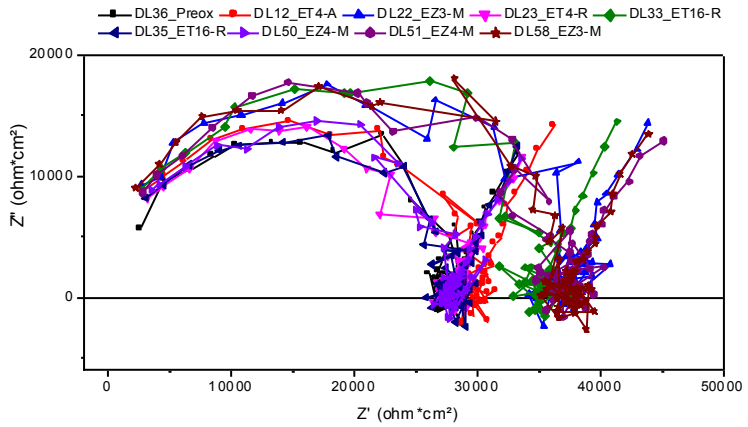

Figure 2. EIS diagrams of preoxidized 304L SS samples tested at 290°C, 8 MPa and Molar ratio H_2 : O_2 >5. a) Test 1; b) Test 2.

$$Z(\omega) = \frac{R_{CT}}{1 + j \cdot \omega \cdot C \cdot R_{CT}} \qquad (2)$$

where:
Z = Impedance (Ohms-cm^2)
ω = Angular frequency (Radians per second)
R_{CT} = Charge transfer resistance (Ohms)
j = Complex number
C = Capacitance (Farads)

$$C = \frac{\varepsilon \cdot \varepsilon^0 \cdot A}{\delta} \qquad (3)$$

where:
ε^0 = Vacuum permittivity
ε = Dielectric material
A = Area of the Plates
δ = Thickness

Table V. Capacitance of preoxidized 304L SS tested at 290°C, 8 MPa and Molar ratio H_2 : O_2 >5 (Test 1).

Sample ID	Re (kΩ)	R_{CT} (kΩ)	Capacitance (μF)
DL36 Preox	0.44	25.21	33
DL12 ET4-A	0.72	28.23	30
DL23 ET4-R	0.86	23.39	47
DL33 ET16-R	0.99	27.88	39
DL35 ET16-R	0.86	25.42	49
DL22 EZ3-M	1.14	28.23	57
DL58 EZ3-M	0.79	28.02	38
DL50 EZ4-M	0.86	23.18	43
DL51 EZ4-M	0.99	25.21	68

Table VI. Capacitance of preoxidized 304L SS tested at 290°C, 8 MPa and Molar ratio H_2 : O_2 >5 (Test 2).

Sample ID	Re (kΩ)	R_{CT} (kΩ)	Capacitance (μF)
DL36 Preox	1.16	27.10	93
DL12 ET4-A	0.77	29.30	42
DL23 ET4-R	0.59	28.44	35
DL33 ET16-R	0.77	35.12	15.1×10^3
DL35 ET16-R	0.56	28.44	123
DL22 EZ3-M	0.47	37.03	102
DL58 EZ3-M	0.59	37.03	43
DL50 EZ4-M	0.59	28.44	44
DL51 EZ4-M	0.59	37.03	2.38×10^{-3}

3.2 Surface Characterization

In Figure 3 we present the chemical maps obtained by EDX in the SEM, in low amplification (40X), to identify the homogeneity of the studied deposits. We note that almost the full area is coated by Ti or Zr, with exception of the samples DL50 and DL51. We observe some differences between samples with the same kind of deposit, as the samples DL33 and DL35, where the surface of the last one seems smoother than the surface of DL33. In the same way, the sample DL50 has a less coated area than DL51. Such observations have a relationship with the electrochemical results discussed previously, but also with the results obtained by XRD (see Figure 4), as discussed below.

TiO_2

Focusing us un the surface analysis of the TiO_2 nanodeposits and relating them with the electrochemical results, we may comment the following:

Anatase
According the XRD patterns of the sample DL12 (see Figure 4 a)), the nanodeposit is very thin, since it is only detected the matrix of 304L SS. Neither we detect any phase (Fe_3O_4, Fe_2O_3 or γFe_2O_3) produced during the preoxidized process to which the sample was submitted, however this deposit present the lower CR in Test 1 and Test 2, but also the lower i_{corr} and higher Rp in Test 2 (after the longer time, 26 days, in the studied environmental conditions).

Rutile
According with the intensity of the XRD peak at $2\theta=27.495°$, corresponding to the plane (110) of rutile, from Figure 4 a) we observe that the sample DL23 has the thicker nanodeposit. This sample also present the more uniform deposit as we may see in Figure 3. However, that is not enough to provide a beneficial effect to 304L SS since both, i_{corr} and CR increases with this deposit. The samples DL33 and DL35, with a less thick deposit, present the same behavior and Rp increases, but i_{corr} and CR decreases when we compare the results with the preoxidized sample (DL36).

ZrO_2

From Figure 4 b), from the intensity of the XRD peak at $2\theta= 28.218$, plane (111) of monoclinic ZrO_2, the nanodeposit with the higher thickness is the one of the sample DL51, which is non uniform (see Figure 3). As per LPR technique, this sample present a slightly better electrochemical behavior than the preoxidized sample (see Table III and Table IV). Concerning the samples DL22 and DL58, they present a slightly difference in the thickness of the deposit (Figure 4 b)), being thinner in sample DL58. This difference in thickness produced a little decrease in the electrochemical behavior of sample DL58, however for practical purposes both samples has the same answer in LPR and EIS.

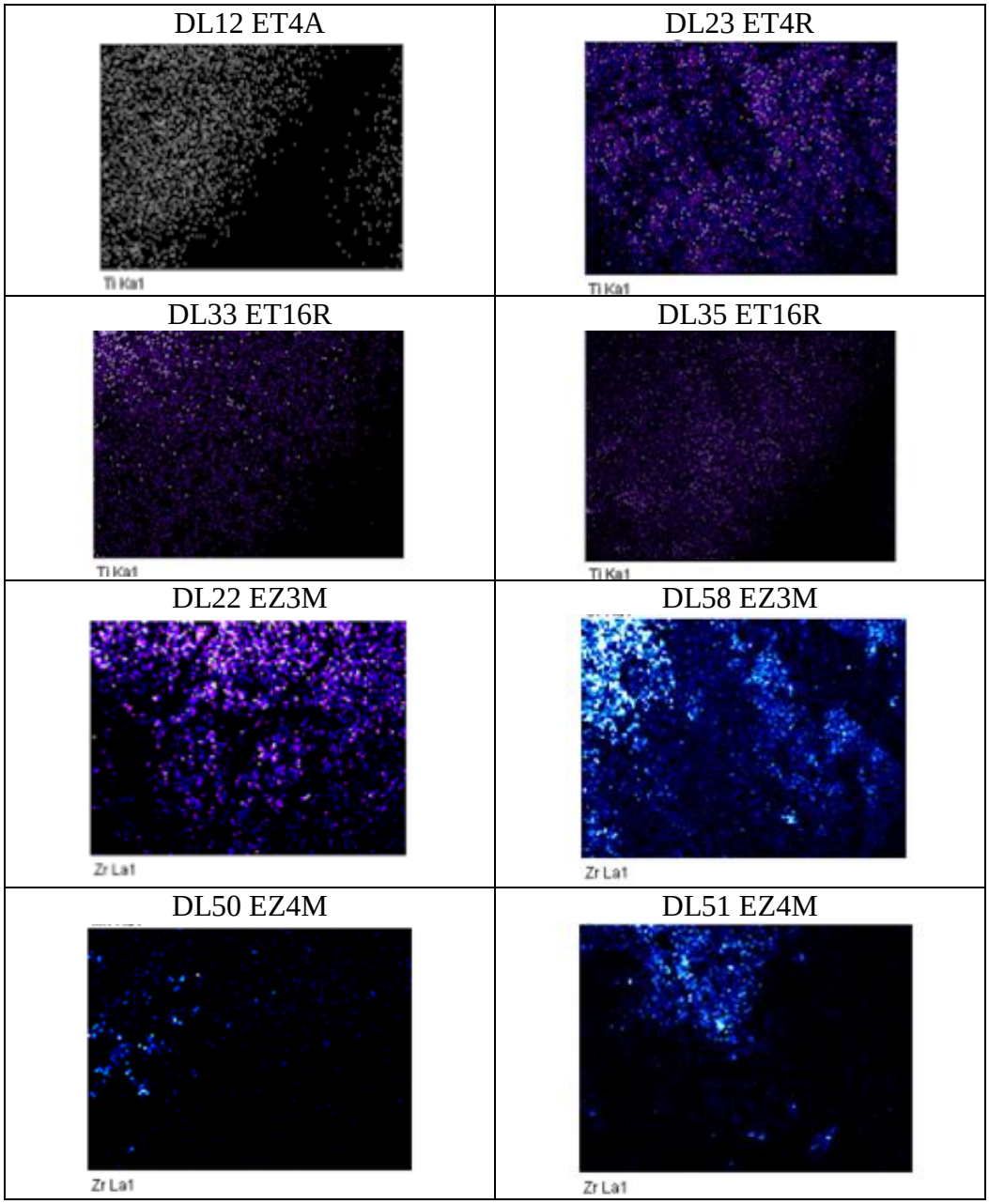

Figure 3. Chemical maps, obtained at 40X by EDX in SEM, of Zr and Ti distribution on the Surface of the samples of preoxidized 304L SS with ceramic nanodeposits of TiO_2 y ZrO_2.

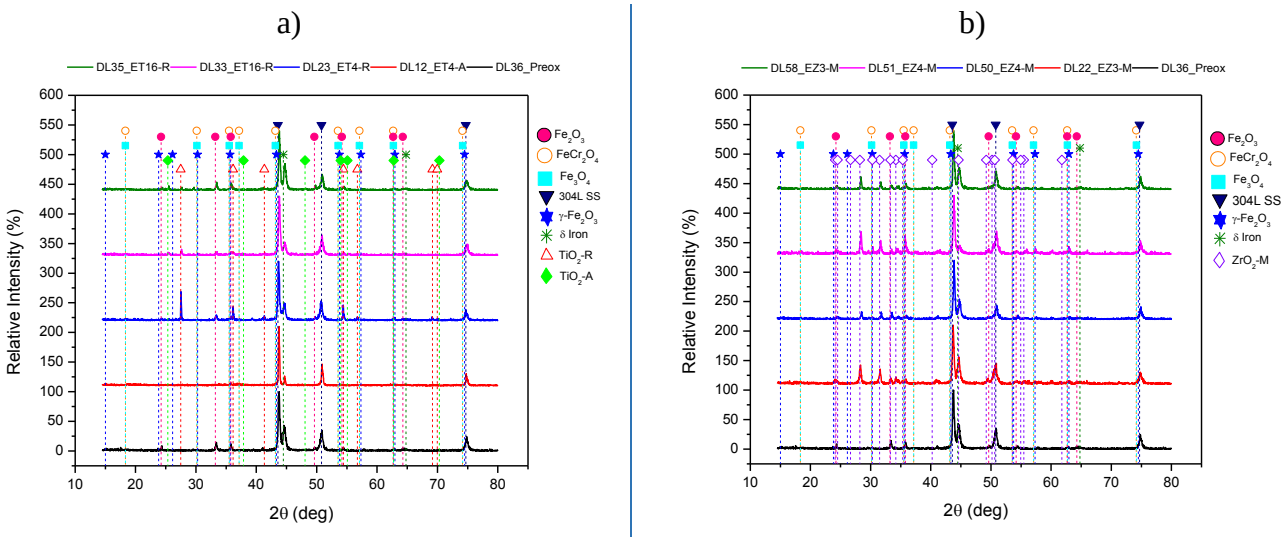

Figure 4. XRD patterns of preoxidized 304L SS with ceramic nanodeposits a) TiO_2 y b) ZrO_2.

4. CONCLUSIONS

As per LPR and EIS tests, nanodeposits of TiO_2 and ZrO_2 have a positive effect in the electrochemical kinetic parameters that could affect the SCC susceptibility of 304L SS at 290°C and 8 MPa. Such nanodeposits decrease CR and i_{corr} of preoxidized 304L SS, at the time that increase Rp and R_{CT}. Two conditions must be fulfilled on order to obtain such results: the deposit must be homogenous and thin.

In the studied environmental conditions (molar ratio $H_2 : O_2 > 5$), TiO_2 and ZrO_2 nanodeposits increase the ECP of 304L SS.

To determine the effect of the studied deposits in the kinetics of SCC, they must be used in SCC tests, such as Slow Strain Rate Tests (SSRT) or crack growth tests.

ACKNOWLEDGMENTS

Financial support of the project ININ CA-218 is gratefully acknowledged. This work has been as well supported by CONACyT through the fellowship number 326110.

REFERENCES

1. C. Lemaignan, "Structural Materials under irradiation", in notes of "*The 2006 Fréderic Joliot & Otto Hann summer School on Nuclear Reactors: challenges and Innovation for light water reactors*", Cadarache, France 23 August- 1 September 2006.
2. T. Onchi, K. Dohi, N. Soneda, Marta Navas, M.L. Castaño, "Mechanism of irradiation assisted stress corrosion crack initiation in thermally sensitized 304 stainless steel", J. Nucl. Mats., **340** (2005) 219-236.
3. Y.-J. Kim, P.L. Andresen, "Transformation Kinetics of Oxide formed on noble Metal-treated type 304 Stainless Steel in 288°C Water", Corrosion NACE International, **59** (2003) 511-519.

4. P.L. Andresen, "Stress Corrosion Cracking (SCC) of ausntenitic stainless steels in high temperature light water ractor (LWR) environments", in *Understanding and Mitigating Ageing in nuclear power plants: Materials and operational aspects of plant life management (PLiM)*, Edited by Philip G. Tipping, Woodhead Publishing (2010) pp. 236-307.
5. S.E. Garcia, P. Tran, J.F. Giannelli, A.J. Jarvis, M.L. Jarvis, "BWR Source Term Management – Strategies and Results at General Electric-designed BWRs", *2010 ISOE International Symposium*, Cambridge (United Kingdom), 17-19 November 2010.
6. http://us.areva.com/home/liblocal/docs/Catalog/BWR/ANP_U_485_V1_14_ENG_MethanolInjectionTechnolgy.pdf
7. Tsung-Kuang Yeh, Yu-Jen Huang, Mei-Ya Wang, Chuen-Horng Tsai, Hydrothermal treatments of TiO_2 on Type 304 stainless steels for corrosion mitigation in high temperature pure water, Nuclear Engineering and Design, **254** (2013) 228– 236.
8. T.K. Yeh, C.H. Tsai, "Intergranular Stress Corrosion Cracking of Platinum Treated type 304 stainless steel in high temperature water", Journal of Nuclear Science and Technology, **41** (2004) 116-125.
9. A. Díaz Sánchez, P. Fuentes Castañeda, F. Merino Caballero, V. Castaño Meneses, "Propagación de grietas en Acero Inoxidable AISI 304L en condiciones de Química de Hidrógeno (HWC)", *in proceedings of XVI Congreso Técnico-Científico ININ-SUTIN*, Centro Nuclear Nabor Carrillo, Mexico, 6-8 September 2006.
10. R. Cottis, S. Turgoose, *Electrochemical Impedance and Noise*, NACE International (1999).
11. S. Tait, *An introduction to electrochemical corrosion testing for practicing engineers and scientists*, PairODocs Publications. Wisconsin, EUA (1994).
12. G. Brug, G. Van den Eeden, M. Sluyters-Rehbach, J. Sluyters, Journal Electroanalytical Chemistry, **176** (1984) 275-295.